DEUTSCHES ELEKTRONEN-SYNCHROTRON DESY

DESY 74/46
September 1974

Backward Production of π^0 by Virtual Photons

by

T. Azemoon, D. Lüke, G. Specht
Deutsches Elektronen-Synchrotron DESY, Hamburg

H. Ackermann, E. Ganßauge
Universität Marburg

F. Janata, D. Schmidt
Bergische Universität
Gesamthochschule Wuppertal

2 HAMBURG 52 · NOTKESTIEG 1

To be sure that your preprints are promptly included in the
HIGH ENERGY PHYSICS INDEX ,
send them to the following address (if possible by air mail) :

DESY
Bibliothek
2 Hamburg 52
Notkestieg 1
Germany

BACKWARD PRODUCTION OF π^0 BY VIRTUAL PHOTONS

T. Azemoon, D. Lüke, G. Specht
Deutsches Elektronen-Synchrotron DESY

H. Ackermann, E. Ganßauge
Universität Marburg

F. Janata, D. Schmidt
Bergische Universität
Gesamthochschule Wuppertal

Abstract

Electroproduction of π^o in backward direction with respect to the virtual photon is measured in a two-arm spectrometer. Cross sections for the reaction $\gamma_v p \to \pi^o p$ are given as functions of q^2, W and θ^* in the regions

$$0.1 < |q^2| < 0.9 \text{ GeV}^2$$

$$1.7 < W < 2.5 \text{ GeV}$$

$$145 < \theta^* < 180^o .$$

1. Introduction

In this paper we report on electroproduction of π^o on protons,

$$e\ p \rightarrow e\ \pi^o\ p \qquad (1)$$

in backward direction with respect to the exchanged virtual photon. The cross section was measured in the following kinematical region:

$$1.7 < W < 2.5\ \text{GeV}$$

$$0.1 < |q^2| < 0.9\ \text{GeV}^2$$

$$145 < \theta^* < 180^o$$

$$0 < \phi < 360^o\ .$$

The scattered electron and proton were detected in coincidence in two spark chamber spectrometers. The electron was identified by Čerenkov and shower counters. The proton was identified by a Čerenkov counter (which separated against high energy pions) and a time-of-flight measurement system (which separated against kaons and low energy pions). Details of the apparatus have been described in ref. 1.

2. Kinematics

The following notations are used:

e, e', γ_v, p, p'	are the four-momenta of the particles: the primary and the scattered electron, the virtual photon, the target and the scattered proton.
$W^2 = (\gamma_v + p)^2$	mass squared of the $\gamma_v p$ system.
$q^2 = (e - e')^2$	mass squared of the virtual photon γ_v.
θ^*	polar angle between p and p' in the CMS.
ϕ	azimuthal angle of the scattered proton p'. ϕ is the angle between the polarization plane (subtended by e and e') and the production plane (subtended by γ_v and p').

Assuming one-photon exchange one obtains the equation

$$\frac{d^4\sigma}{dq^2\, dW^2\, d\cos\theta^*\, d\phi} = \Gamma \left\{ \frac{d\sigma_u}{d\cos\theta^*} + \varepsilon \frac{d\sigma_L}{d\cos\theta^*} + \varepsilon \frac{d\sigma_P}{d\cos\theta^*} \cos 2\phi + \right.$$

$$\left. + \sqrt{2\,\varepsilon(\varepsilon+1)}\ \frac{d\sigma_I}{d\cos\theta^*}\ \cos\phi \right\} \qquad (2)$$

which connects the measured cross section of the reaction $ep \to e\pi^o p$ (left hand side of equ. 2) with the virtual photon cross section of the reaction $\gamma_v p \to \pi^o p$ (right hand side of equ. 2).

In the limit $q^2 \to 0$ the virtual photon cross section approaches the cross section for unpolarized real photons. The term σ_u is the cross section for unpolarized transverse virtual photons; σ_p is due to transverse linear polarization; σ_L accounts for longitudinal photons; and σ_I is the interference between the transverse and the longitudinal components. Γ is the flux of the virtual photons; ε is the transversal polarization. In this experiment ε varies in the range $0.7 < \varepsilon < 0.9$. Because of the small range of ε, σ_u and σ_L cannot be determined separately.

Data have been taken at primary electron energies of 4.0 and 4.9 GeV. Fig. 1 shows the regions of W and q^2 covered by the data. One has to distinguish three kinematical regions corresponding to different ranges of the azimuthal angle ϕ accepted by our apparatus. In region A all angles $0^o < \phi < 360^o$ are accepted. In this region we studied the ϕ dependence according to equ. 2. In regions B and C the acceptance is limited to $150^o < \phi < 210^o$ and $-120^o < \phi < +120^o$, respectively. In both regions B and C we averaged the cross section over the accepted ϕ interval.

3. Data Analysis

66000 and 72000 events with an observed proton in the final state have been measured at the two values of the primary electron energy $E_o = 4.0$ and 4.9 GeV. For events with $E_o = 4.0$ GeV Fig. 2 shows the spectrum of the missing mass squared M^2, not

corrected for acceptance. π^o production via reaction $\gamma_v p \to \pi^o p$ and ρ^o and ω production via reactions $\gamma_v p \to \rho^o p$ and ωp show up as clear peaks in the missing mass spectrum.

Events of the reaction $\gamma_v p \to \pi^o p$ were identified by a cut in the missing mass squared $-0.08 < M^2 < 0.10$ GeV^2 (for $E_o = 4.0$ GeV) and $-0.08 < M^2 < 0.15$ GeV^2 (for $E_o = 4.9$ GeV). In these regions 2930 resp. 605 events were found for the two primary energies. To calculate the cross section these events have been weighted for the acceptance of our apparatus. The cross section was corrected for the fraction of π^o contribution in the mentioned missing mass range. The π^o fraction was determined by a fit of a Gaussian distribution for the π^o (with a width $\sigma = 0.02 - 0.04$ GeV^2 depending on the kinematics) and a polynomial for the background. For different kinematical points we found different π^o fractions variing between 50 % and 95 %.

The cross section was also corrected for losses due to the cut in the missing mass ($\lesssim$ 5 %), for efficiency losses in the trigger, Čerenkov and shower counters ($\simeq$ 6 %), for loss of events by the automatic data analysis procedure ($\simeq$ 10 %). Radiative corrections variing from 15 % to 20 % have been applied.

The uncertainties in these corrections add up to an overall systematic error of about $\pm$10 % which is not included in the errors given in the figures. The data analysis is discussed in more detail in ref. 2.

4. Results

The differential cross sections for the reaction $\gamma_v p \to \pi^o p$ as function of W, θ^* and q^2 are shown in Figs. 3, 4 and 5.

The cross sections denoted by $d\sigma/d\Omega$ are the values of $d(\sigma_u + \varepsilon \sigma_L)/d\cos\theta^*$, $d\sigma_p/d\cos\theta^*$ and $d\sigma_I/d\cos\theta^*$ which have been divided by the factor 2π in order to allow a comparison with photoproduction cross sections $d\sigma_u/d\Omega$.

In the kinematical region A where we accepted all ϕ angles, the ϕ dependence of the cross section turned out to be very flat. This means that the values of $d\sigma_I/d\Omega$ and $d\sigma_p/d\Omega$ are small ($\simeq$ 10 % of $d(\sigma_u + \varepsilon \sigma_L)/d\Omega$), and, moreover, they are compatible with zero (see Fig. 5). In the kinematical regions B and C the ϕ dependence could not be studied. Therefore the cross sections $d\sigma/d\Omega$ averaged over the covered ϕ interval are given in the figures.

The W dependence of the cross section $d\sigma/d\Omega$ is shown in Fig. 3 at $|q^2| = 0.35$ GeV^2 and a backward production angle of $\theta^* = 150^\circ$. The values show a resonance peak around W = 1.9 GeV. For comparison the photoproduction cross section[3] measured at $\theta^* = 180^\circ$ is given, which also shows a significant resonant structure around W = 1.9 GeV. In photoproduction of πN states the excitation of a nucleon resonance with mass around 1.9 MeV is assumed[4], with a dominating amplitude $\lambda = 1/2$ for the initial helicity which results in an increasing $\pi^\circ p$ cross section when θ^* increases to 180°.

The θ^* dependence found in this experiment is given in Fig. 4 for two W regions. According to the resonance structure seen in Fig. 3 data below and above W = 2.1 GeV are analyzed separately. In both W regions the cross section increases to the backward direction.

In Fig. 5 the cross section $d\sigma/d\Omega$ is given as a function of q^2 for two kinematical points ($\overline{W}$ = 1.9 GeV, 2.25 GeV; $\overline{\theta^*} = 165^\circ$, 170°). At these values of W and θ^* no photoproduction measurements exist. Therefore the photoproduction value measured at $\theta^* = 180^\circ$ (ref. 3) have been scaled to the angles $\theta^* = 165^\circ$ resp. 170° assuming that the θ^* dependence as observed for virtual photons (Fig. 4) is also valid for real photons. In Fig. 5 the results of the CEA-electroproduction experiment[5] at a somewhat different kinematical point ($1.9 < W < 2.0$ GeV, $\theta^* \sim 167^\circ$) are also shown. The results of both electroproduction experiments show the general tendency of a decreasing cross section with increasing $|q^2|$. For eyeguidance the prediction of a simple VDM ($\sim(m_\rho^2 - q^2)^{-2}$), scaled to the photoproduction value, is given by the curve in Fig. 5. If one assumes VDM to be correct and $d\sigma_I/d\Omega$ and $d\sigma_P/d\Omega$ to be neglectable, the contribution of $d\sigma_L/d\Omega$ is small compared with $d\sigma_u/d\Omega$, a result which agrees with the measurement of the total cross section in this W region.

5. Summary

Backward production of π° by virtual photons shows a resonance structure at $W \approx 1.9$ GeV. The cross section increases when θ^* goes to 180°. No hint for a σ_L contribution could be found in the data.

Acknowledgements

We wish to thank Drs. I. Dammann, C. Driver and K. Heinloth for valuable cooperation and Mr. G. Augustinski, Mr. P. Burmeister, Mr. K. Maschidlauskas, Mrs. B. Nissen and Mrs. R. Siemer for their excellent assistance. The superior performance of the Synchrotron crew, the Hallendienst, the Kältetechnik and the Rechenzentrum is gratefully acknowledged.

Literature

1) T. Azemoon et al., Production of Hyperons by Virtual Photons, DESY Report 74/45.

2) C. Driver et al., Nucl. Phys. B30, 245 (1971).

3) G. Buschhorn et al., Phys. Rev. Letters 20, 230 (1968).

4) R.L. Walker, 1969 International Symposium on Electron and Photon Interactions at High Energies, Liverpool, 1969, p. 23.

5) C.N. Brown et al., 1971 International Symposium on Electron and Photon Interactions at High Energies, Cornell, 1971, p. 336 (contribution No. 273).

Figure Captions

1) Acceptance range q^2 vs. W of the apparatus for two different energies E_o of the primary electron.

2) Spectrum of the missing mass squared M^2 obtained with a primary electron energy of 4.0 GeV. The spectrum is not corrected for acceptance.

3) Cross section $d\sigma/d\Omega$ as function of W. The photoproduction values were taken from ref. 3.

4) Cross section $d\sigma/d\Omega$ as function of θ^*.

5) Cross sections $d\sigma/d\Omega$ resp. $d\sigma_u/d\Omega + \varepsilon\, d\sigma_L/d\Omega$, $d\sigma_I/d\Omega$ and $d\sigma_P/d\Omega$ as functions of q^2. For $1.7 < W < 2.1$ GeV, values marked as ⧫ were obtained in kinematical region B, ⊔ were measured in region A and scaled to $W = 1.9$ GeV using the known W dependence (Fig. 3), ⊙ were taken from ref. 5. For $2.1 < W < 2.4$ GeV the values were obtained in kinematical region C. Photoproduction data are based on the results of ref. 3. The curves show the VDM prediction $\sim(0.58 - q^2)^{-2}$ normalized to the photoproduction values.

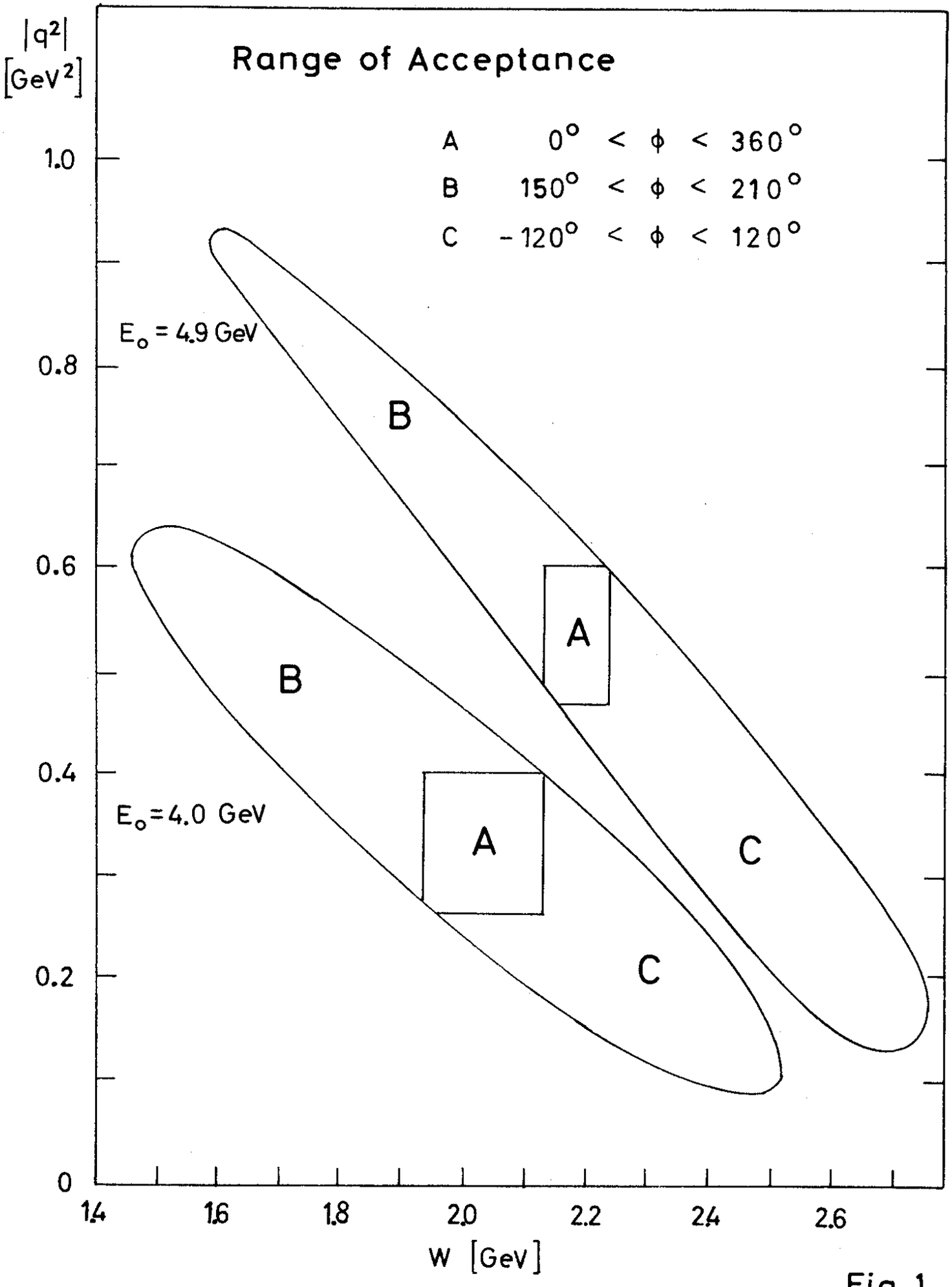
Range of Acceptance
A 0° < φ < 360°
B 150° < φ < 210°
C -120° < φ < 120°
|q²| [GeV²]
1.0
0.8
0.6
0.4
0.2
0
E₀ = 4.9 GeV
E₀ = 4.0 GeV
A
B
C
A
B
C
1.4
1.6
1.8
2.0
2.2
2.4
2.6
W [GeV]

Fig. 1

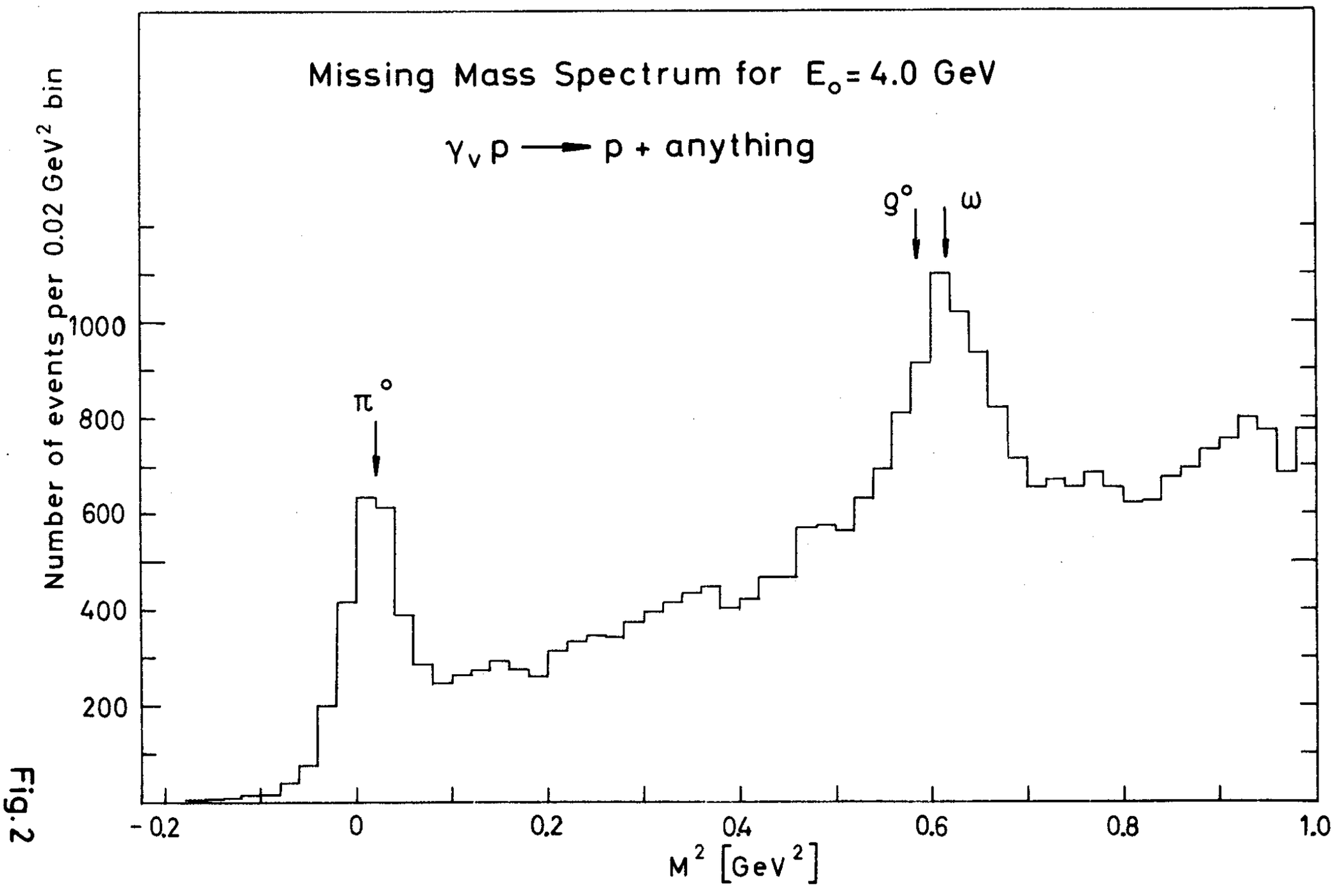
Missing Mass Spectrum for $E_o = 4.0$ GeV
$\gamma_v p \longrightarrow p +$ anything
ϱ°
ω
π°
Number of events per 0.02 GeV^2 bin
1000
800
600
400
200
-0.2
0
0.2
0.4
0.6
0.8
1.0
M^2 [GeV^2]

Fig. 2

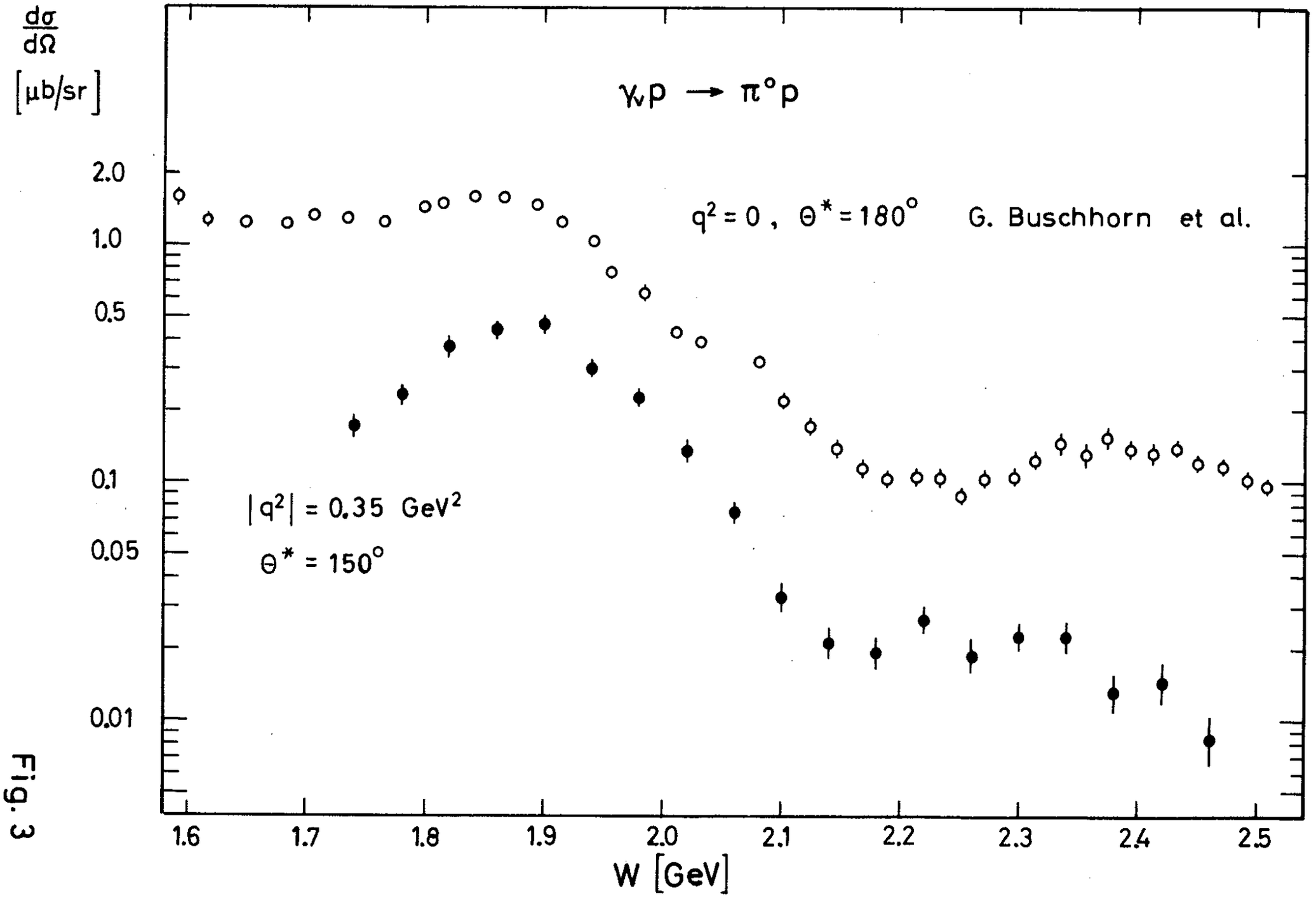
dσ/dΩ
[μb/sr]
γvp → π°p
q² = 0 , Θ* = 180°
G. Buschhorn et al.
|q²| = 0.35 GeV²
Θ* = 150°
2.0
1.0
0.5
0.1
0.05
0.01
1.6
1.7
1.8
1.9
2.0
2.1
2.2
2.3
2.4
2.5
W [GeV]

Fig. 3

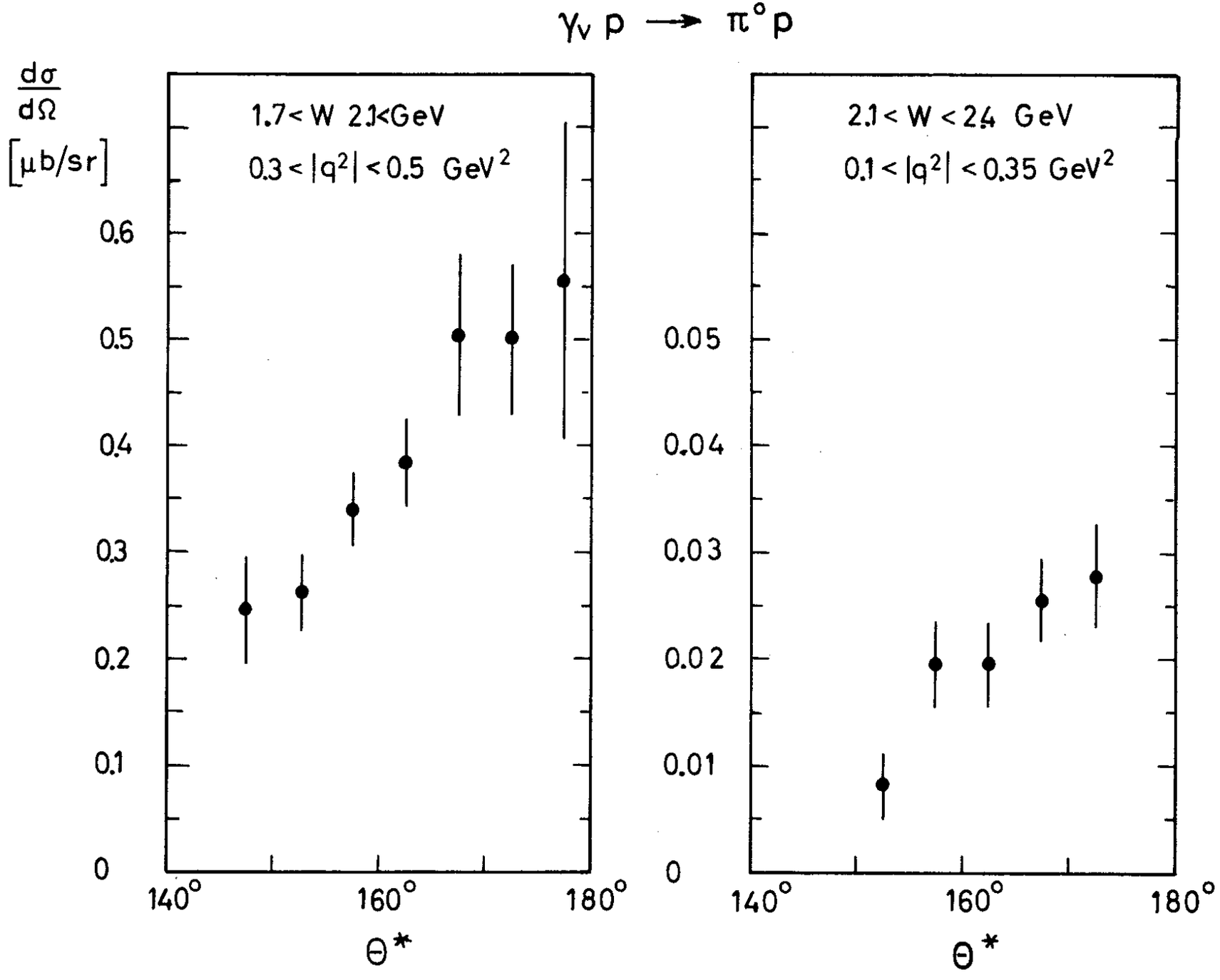
$\gamma_v p \rightarrow \pi^\circ p$
$\frac{d\sigma}{d\Omega}$
[μb/sr]
1.7< W 2.1<GeV
0.3 < |q²| < 0.5 GeV²
2.1 < W < 2.4 GeV
0.1 < |q²| < 0.35 GeV²
0.6
0.5
0.4
0.3
0.2
0.1
0
0.05
0.04
0.03
0.02
0.01
140°
160°
180°
Θ*

Fig. 4

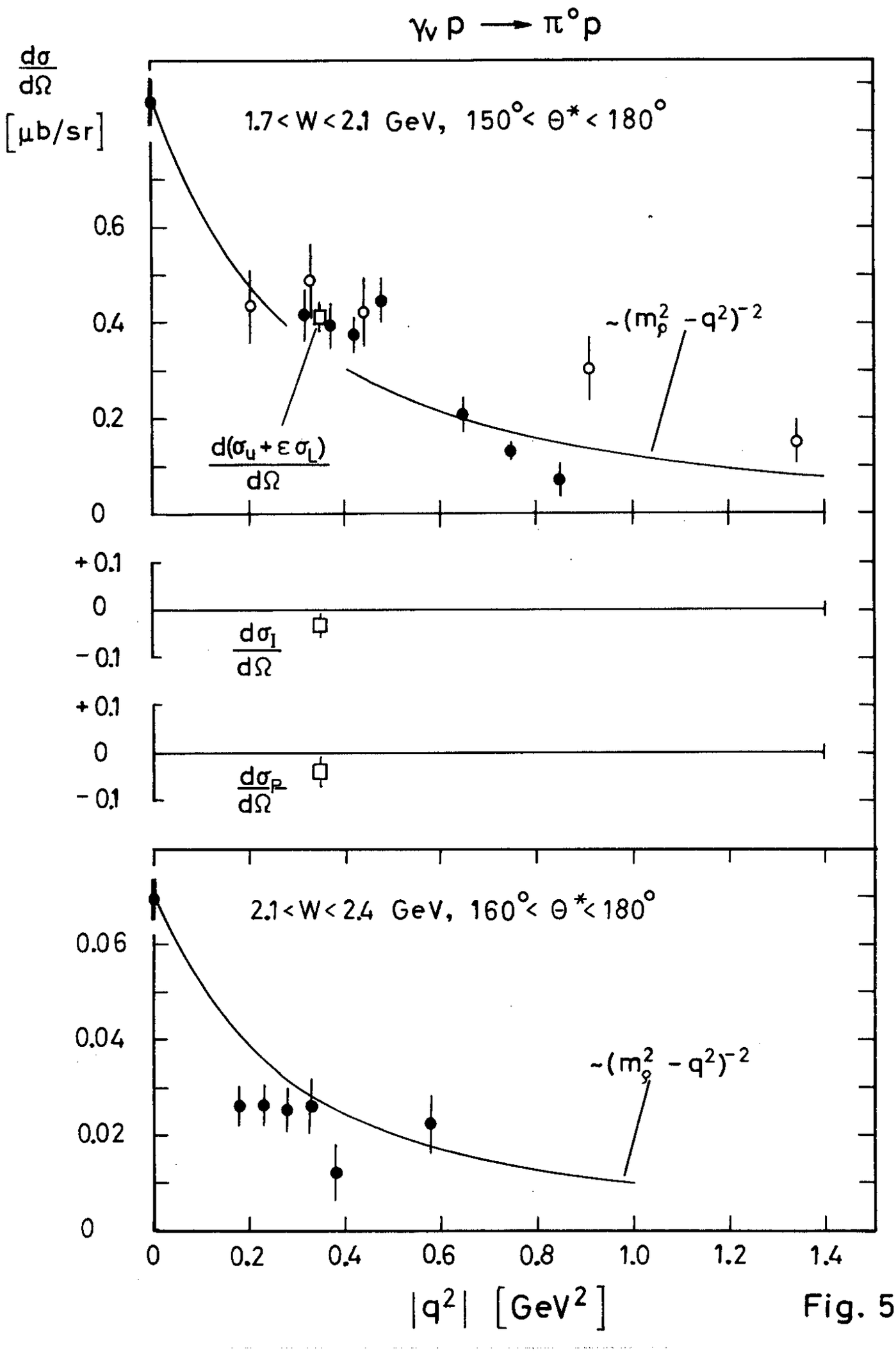
γv p → π°p
dσ/dΩ
[μb/sr]
1.7 < W < 2.1 GeV, 150° < Θ* < 180°
0.6
0.4
0.2
0
~(m_ρ² − q²)⁻²
d(σ_u + ε σ_L)/dΩ
+0.1
0
−0.1
dσ_I/dΩ
+0.1
0
−0.1
dσ_P/dΩ
2.1 < W < 2.4 GeV, 160° < Θ* < 180°
0.06
0.04
0.02
0
~(m_ρ² − q²)⁻²
0
0.2
0.4
0.6
0.8
1.0
1.2
1.4
|q²| [GeV²]

Fig. 5